Observation of Quasiparticle Pair Production and Quantum Entanglement in Atomic Quantum Gases Quenched to an Attractive Interaction

Cheng-An Chen, Sergei Khlebnikov, and Chen-Lung Hung

Phys. Rev. Lett. **127**, 060404 — Published 6 August 2021

DOI: 10.1103/PhysRevLett.127.060404

Observation of quasiparticle pair-production and quantum entanglement in atomic quantum gases quenched to an attractive interaction

Cheng-An Chen,[1] Sergei Khlebnikov,[1,2] and Chen-Lung Hung[1,2,*]

[1] *Department of Physics and Astronomy, Purdue University, West Lafayette, IN 47907, USA*
[2] *Purdue Quantum Science and Engineering Institute, Purdue University, West Lafayette, IN 47907, USA*

(Dated: July 7, 2021)

We report observation of quasiparticle pair-production by a modulational instability in an atomic superfluid and present a measurement technique that enables direct characterization of quasiparticle quantum entanglement. By quenching the atomic interaction to attractive and then back to weakly repulsive, we produce correlated quasiparticles and monitor their evolution in a superfluid through evaluating the in situ density noise power spectrum, which essentially measures a 'homodyne' interference between ground state atoms and quasiparticles of opposite momenta. We observe large amplitude growth in the power spectrum and subsequent coherent oscillations in a wide spatial frequency band within our resolution limit, demonstrating coherent quasiparticle generation and evolution. The spectrum is observed to oscillate below a quantum limit set by the Peres-Horodecki separability criterion of continuous-variable states, thereby confirming quantum entanglement between interaction quench-induced quasiparticles.

Coherent pair-production processes are enabling mechanisms for entanglement generation in continuous variable states [1, 2]. In many-body systems, quasiparticle pair-production presents an interesting case, as interaction creates entanglement shared among collectively excited interacting particles. Entanglement distribution through quasiparticle propagation is a direct manifestation of transport property in a quantum many-body system [3, 4]. Controlling quasiparticle pair-production and detecting entanglement evolution thus opens a door to probing quantum many-body dynamics, enabling fundamental studies such as information propagation [5, 6], entanglement entropy evolution [7], many-body thermalization [8], as well as Hawking radiation of quasiparticles and thermodynamics of an analogue black hole [9–11].

In atomic quantum gases, coherent quasiparticle pair-production can be stimulated through an interaction quench, which results in a rapid change of quasiparticle dispersion relation that can project collective excitations, from either existing thermal or quantum populations, into a superposition of correlated quasiparticle pairs [12–14]. This has led to a prior observation of Sakharov oscillations in a quenched atomic superfluid [13, 15]. However, direct verification of quasiparticle entanglement has remained an open question.

An intriguing case occurs when the atomic interaction is quenched to an attractive value. In that case, not only a larger change of quasiparticle dispersion is involved, there is also an unstable band, in which quasiparticle dispersion $\epsilon(k)$ is purely imaginary, $\epsilon^2(k) < 0$, where k is the momentum wavenumber. As a consequence, the early time dynamics is governed by a modulational instability (MI), which continuously stimulates production of quasiparticle pairs, and the ground state becomes unstable with respect to an exponential growth of density waves. This growth leads eventually to wave fragmentation and soliton formation [16]. Although these consequences of MI have been observed [17–21], the early-time evolution itself has only been recently studied [21]. Nevertheless, it is precisely the early-time dynamics that promises MI-enhanced pair-production and quantum entanglement. We note there is a parallel scheme using a roton instability for enhanced quasiparticle entanglement generation in dipolar quantum gases [22].

In this letter, we demonstrate MI-enhanced coherent quasiparticle pair-production in a homogeneous 2D quantum gas quenched to an attractive interaction, and report an in situ detection method that enables direct characterization of quasiparticle entanglement beyond an existing method [9, 23]. Specifically, we monitor coherent quasiparticle evolution after quenching the interaction back to a positive value (see Fig. 1 for protocol). Through in situ imaging, we analyze the dynamics of density observables by a method analogous to the well-established homodyne detection technique in quantum optics [24–26] and confirm non-classical correlations, that is, quantum entanglement in quasiparticle pairs.

Our analyses are based on the time evolution of in situ density noise, which is a manifestation of interference between quasiparticle excitations and the ground state atoms that serve as a coherent local oscillator [28]. In Fourier space, the density noise operator can be written as $\delta\hat{n}_{\mathbf{k}} \approx \sqrt{N}(\hat{a}^\dagger_{\mathbf{k}} + \hat{a}_{-\mathbf{k}})$, where $N \gg 1$ is the total atom number nearly all accounted for by the ground state atoms, and $\hat{a}^{(\dagger)}_{\pm\mathbf{k}}$ are the annihilation (creation) operators for $\pm\mathbf{k}$ single-particle momentum eigenstates. They are related to quasiparticle operators $\hat{\alpha}^\dagger_{\pm\mathbf{k}}$ by the Bogoliubov transformation. We study the density noise power spectrum $S(\mathbf{k}) = \langle|\delta n_{\mathbf{k}}|^2\rangle/N$, where $\langle\cdots\rangle$ denotes ensemble averaging. Within our resolution limit ($|\mathbf{k}| \lesssim 2.6/\mu$m), the power spectrum conveniently measures the combined variance of two-mode ($\pm\mathbf{k}$) quasi-

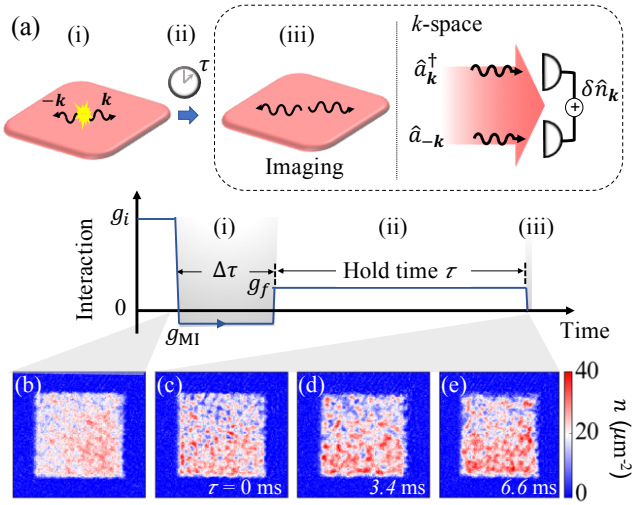

FIG. 1. Experiment scheme for quasiparticle pair-production and detection. (a) A homogeneous 2D superfluid (red square) undergoes an interaction quench protocol from (i) $g = g_i > 0$ to $g_{\rm MI} < 0$ for broadband generation of quasiparticle pairs of opposite momenta (illustrated by black curvy arrows) for a time duration $\Delta\tau$; (ii) A second interaction quench to $g = g_f > 0$ allows quasiparticles to evolve as phonons for a variable hold time τ; (iii) In situ density noise in spatial frequency domain, $\delta n_{\mathbf{k}}$, is essentially a 'homodyne' measurement of excitations in opposite momentum states interfering with ground state atoms. (b-e) Single-shot density images taken prior to (b) or after the interaction quench (c-e) and held for the indicated time τ. Image size: 77×77 μm^2.

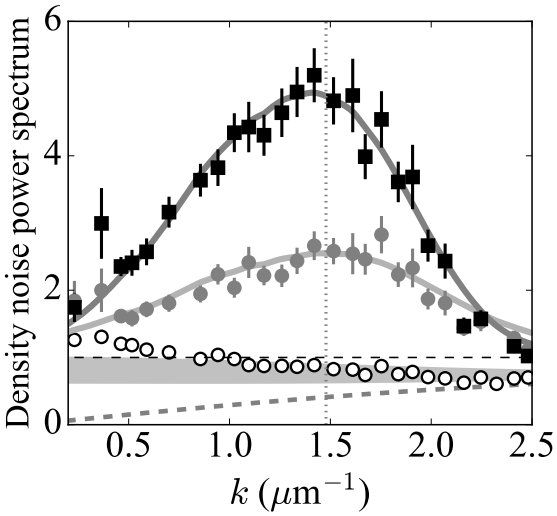

FIG. 2. Growth of density noise during the MI period. Density noise power spectra measured before, $S_0(k)$ (open circles), and right after the MI period, $S(k,0)$, with $\Delta\tau \approx 1$ ms (gray circles) and 2 ms (black squares), respectively. Horizontal dashed line marks the atomic shot-noise level. Gray band represents calculated initial phonon spectrum assuming equilibrium temperature $T = 8 \pm 2$ nK. Dashed curve shows the squeezing parameter C_k at $g = g_i \approx 0.127$. Solid curves are theory fits to data; see text [27]. Vertical dotted line marks the wavenumber k_c, below (above) which quasiparticles are expected to be unstable (stable) at $g = g_{\rm MI} \approx -0.026$.

particle quadrature operators $\hat{x}_{\mathbf{k}} + \hat{x}_{-\mathbf{k}}$ and $\hat{p}_{\mathbf{k}} - \hat{p}_{-\mathbf{k}}$, where $\hat{x}_{\mathbf{k}} = (\hat{\alpha}^\dagger_{\mathbf{k}} + \hat{\alpha}_{\mathbf{k}})/\sqrt{2}$ and $\hat{p}_{\mathbf{k}} = i(\hat{\alpha}^\dagger_{\mathbf{k}} - \hat{\alpha}_{\mathbf{k}})/\sqrt{2}$ [27]. Since pair-production should be isotropic in our quantum gas samples, in the following we discuss azimuthally averaged spectrum $S(k)$, and use $\pm k$ to denote opposite momenta. In the superfluid ground state absent quasiparticle (phonon) excitations, the Bogoliubov theory predicts $S(k) = C_k$, where $C_k = \epsilon_k/\epsilon(k,g)$ is the ground-state squeezing parameter, ϵ_k the single-particle energy, $\epsilon(k,g) = \sqrt{\epsilon_k^2 + 2\frac{\hbar^2}{m}\bar{n}g\epsilon_k}$ the phonon dispersion relation, $\bar{n}$ the mean density, g the interaction at the time of the measurement, m the atomic mass, and $\hbar$ the reduced Planck constant.

In the presence of quasiparticles with non-classical correlation, the power spectrum would squeeze below the ground-state level, i.e., to $S(k) < C_k$. This intuitive bound can be formally derived following Refs. [29, 30], which considers a continuous-variable version of the Peres-Horodecki separability criterion for bipartite entanglement. Adapted to our case [27], the criterion states that the variance of two-mode quadratures must satisfy

$$S(k) = \frac{C_k}{2}\left[\langle(\hat{x}_k + \hat{x}_{-k})^2\rangle + \langle(\hat{p}_k - \hat{p}_{-k})^2\rangle\right] \geq C_k\,, \quad (1)$$

in the absence of quasiparticle entanglement. For non-interacting atoms ($g = 0$), $C_k = 1$, and the above inequality represents the limit of atomic shot-noise. For phonons in a superfluid ($g > 0$), the separability criterion requires a lower limit ($C_k < 1$).

In the final state of our quench protocol ($g > 0$), coherent quasiparticle pairs interfere and $S(k)$ should be time-dependent. In the special case of noninteracting phonons, that dependence has the form

$$S(k,\tau) = C_k\left[1 + \bar{N}_k + \Delta N_k \cos\phi_k(\tau)\right], \quad (2)$$

where $\bar{N}_k = \langle\hat{\alpha}^\dagger_k\hat{\alpha}_k\rangle + \langle\hat{\alpha}^\dagger_{-k}\hat{\alpha}_{-k}\rangle$ is the mean total phonon number in $\pm k$ modes, $\Delta N_k = 2|\langle\hat{\alpha}_k\hat{\alpha}_{-k}\rangle|$ is the pair correlation amplitude, and $\phi_k(\tau) = 2\epsilon(k,g)\tau/\hbar + \phi_k(0)$ is the argument of $\langle\hat{\alpha}_k\hat{\alpha}_{-k}\rangle$ that evolves at twice the phonon frequency. In this case, violation of the inequality Eq. (1) is equivalent to having $\Delta N_k > \bar{N}_k$ [31, 32]. The presence of maximal two-mode squeezing $S(k)/C_k < 1$ occurs at $\phi_k \approx (2l+1)\pi$, alternating with maximal anti-squeezing $S(k)/C_k > 1$ at $\phi_k \approx 2l\pi$ (l is an integer). In practice, oscillations of $S(k)$ are inevitably damped. Nevertheless, $\pm k$ modes are entangled as long as ΔN_k remains larger than $\bar{N}_k$, or more generally $S(k)$ shows squeezing ($< C_k$) – a key signature that we demonstrate in this letter.

To carry out the experiment, we prepare uniform superfluid samples formed by $N \approx 4.9 \times 10^4$ nearly pure Bose-condensed cesium atoms loaded inside a quasi-2D

box potential, which compresses all atoms in the harmonic ground state along the imaging (z-) direction [21] with $l_z = 184$ nm being the harmonic oscillator length. A time-of-flight measurement estimates the sample temperature $T \lesssim 8$ nK. Mean atomic surface density $\bar{n} \approx 21/\mu\text{m}^2$ is approximately uniform within a horizontal box size of $\approx 48\times48\ \mu\text{m}^2$. The interaction strength of the quasi-2D gas $g = \sqrt{8\pi}a/l_z$ is controlled by the s-wave scattering length a via a magnetic Feshbach resonance [33], giving an initial interaction strength $g = g_i \approx 0.127$. An uncertainty in g ($\delta g \approx \pm 0.0006$) is primarily contributed by the uncertainty in the magnetic field at the scattering length zero-crossing [21].

As illustrated in Fig. 1(a), an MI period is initiated by quenching the atomic interaction (within 0.8 ms) to a negative value $g_{\text{MI}} \approx -0.026$. The quench time scale is short compared to the initial phonon cycle $2\pi\hbar/\epsilon(k, g_i) \gtrsim 2.5$ ms for $k \lesssim 2.6/\mu$m, and the interaction quench is considered quasi-instantaneous. To terminate the MI after additional short hold time $\Delta\tau \approx 1$–2 ms, we quench the atomic interaction back to a small positive value $g_f \approx 0.007$, allowing quasiparticles to evolve as phonons in a stable superfluid for another variable time τ before we perform in situ absorption imaging. We have also analyzed quenches without an MI period ($\Delta\tau = 0$). Figures 1(b-e) show sample images measured before and after we initiate the quench protocol. We evaluate $\delta n_{\mathbf{k}}$ for each sample through Fourier analysis [34] and obtain their density noise power spectra. Typically around 50 experiment repetitions are analyzed for each hold time τ. Each power spectrum has been carefully calibrated with respect to the atomic shot-noise measured from high temperature normal gases [27, 34].

We expect amplified density fluctuations following the MI period due to sudden change of quasiparticle energy dispersion and pair-production [12, 13, 21]. To quantify the growth of density fluctuations, in Fig. 2 we compare the density noise power spectra measured before and immediately after the MI period, that is, for hold time $\tau = 0$. Before MI, the initial spectrum $S_0(k)$ is mostly below the atomic shot-noise due to low temperature $T \lesssim 8$ nK and small initial squeezing parameter $C_k < 1$. Excessive noise in $k \lesssim 0.75/\mu$m may be due to technical heating in the box potential. After the MI time period $\Delta\tau$, we indeed find a significant increase in the density noise, $S(k, 0) > 1$. The growth occurs both in the instability band $k \lesssim k_c = 2\sqrt{\bar{n}|g_{\text{MI}}|} \approx 1.5/\mu$m, where the dispersion $\epsilon(k, g_{\text{MI}})$ is purely imaginary, and in the stable regime $k \gtrsim k_c$ as well. Within these short MI periods, we observe the largest growth near $k \approx k_c$, where $\epsilon(k, g_{\text{MI}}) \approx 0$. We comment that for a much longer MI period, density waves in the instability band eventually dominate the noise power spectrum due to continuously stimulated quasiparticle pairs, as observed in [21].

Our measured spectra can be well-captured by a model that considers coherent evolution from quasiparticle pair-production within the Bogoliubov theory and their damping as well as decoherence due to coupling to single-particle Markovian quantum noise (for details, see Supplemental Information [27]). We refer to the coherent signal in the absence of damping as: $S_{\text{coh}}(k) = S_0(k)[1 + \frac{\epsilon(k,g_i)^2-\epsilon(k,g_{\text{MI}})^2}{\epsilon(k,g_{\text{MI}})^2}\sin^2\frac{\epsilon(k,g_{\text{MI}})\Delta\tau}{\hbar}]$, which describes the hyperbolic growth of density fluctuations in the instability band ($k \lesssim k_c$) [21] and sinusoidal Sakharov oscillations for stable modes ($k \gtrsim k_c$) [13]. On the other hand, quantum noise causes damping (reduction) of the coherent signal and the appearance of an additive incoherent background $S_{\text{inc}}(k)$. The total power spectrum at the end of the MI period is $S(k, 0) = e^{-\Gamma_k\Delta\tau}S_{\text{coh}}(k) + S_{\text{inc}}(k)$, where $S_{\text{inc}}(k) = \frac{1}{2}\{\eta_- \frac{\Gamma_k^2}{\Gamma_k^2+4\epsilon(k,g_{\text{MI}})^2/\hbar^2}[1 - e^{-\Gamma_k\Delta\tau}(\cos\frac{2\epsilon(k,g_{\text{MI}})\Delta\tau}{\hbar} - \frac{2\epsilon(k,g_{\text{MI}})}{\hbar\Gamma_k}\sin\frac{2\epsilon(k,g_{\text{MI}})\Delta\tau}{\hbar})] + \eta_+(1 - e^{-\Gamma_k\Delta\tau})\}$, with $\eta_\pm = 1 \pm \epsilon_k^2/\epsilon(k, g_{\text{MI}})^2$. The coherent and incoherent contributions are coupled by a k-dependent damping rate Γ_k. Our theory fits (solid curves in Fig. 2) suggest $\Gamma_k \sim 0.5\epsilon_k/\hbar$ [27], which is of the same order of

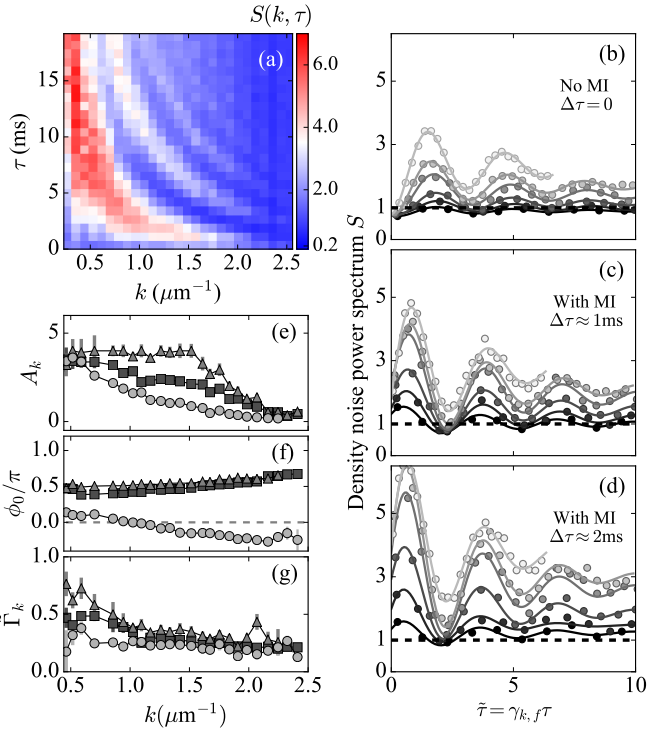

FIG. 3. Coherent oscillations in the density noise power spectrum. (a) Full evolution of the power spectrum $S(k, \tau)$ with $\Delta\tau \approx 1$ ms, showing coherent oscillations in time and k-space. (b-d) Synchronized oscillations of $S(k, \tilde{\tau})$ plotted in the rescaled time unit $\tilde{\tau} = \gamma_{k,f}\tau$ for various $k \approx (1, 1.3, 1.6, 1.8, 2.1, 2.2)/\mu$m (Gray circles from bright to dark). Horizontal dashed lines mark the atomic shot-noise limit. Solid lines are sinusoidal fits. Fitted amplitude A_k, phase offset ϕ_0, and decay rate $\tilde{\Gamma}_k$ from samples with $\Delta\tau \approx 0$ ms (filled circles), 1 ms (filled squares), and 2 ms (filled triangles) are plotted in (e-g), respectively.

magnitude as the decay rate extracted from the subsequent time-evolution measurements at $g = g_f$ (Fig. 3).

To demonstrate phase coherence and pair-correlation in quasiparticles, we plot the complete time and momentum dependence of the density noise power spectrum $S(k, \tau)$, as shown in Fig. 3(a). Here, oscillatory behavior is clearly visible over the entire spectrum. The oscillations are a manifestation of the interference between coherent quasiparticles of opposite momenta $\pm k$, as suggested by Eq. (2), with the relative phase winding up in time as $\phi_k(\tau) = 2\gamma_{k,f}\tau + \phi_0$, where $\gamma_{k,f} = \epsilon(k, g_f)/\hbar$ is the expected Bogoliubov phonon frequency and ϕ_0 is an initial phase difference. In Fig. 3(b-d), we plot $S(k, \tilde{\tau})$ in the rescaled time $\tilde{\tau} = \gamma_{k,f}\tau$ and confirm that all spectra oscillate synchronously with a time period $\approx \pi$, thus validating the phonon interference picture. For comparison, we also plot the evolution of samples with a direct interaction quench from g_i to g_f without an MI period ($\Delta\tau = 0$). Oscillations in $S(k, \tilde{\tau})$ can also be observed, albeit with smaller amplitudes and phase offsets $\phi_0 \approx 0$, as these oscillations result solely from the interference of in-phase quasiparticle projections from suddenly decreasing the Bogoliubov energy [13]. In either case, with or without MI, we observe that phase coherence is lost in a few cycles and the density noise spectra reach new steady-state values.

To quantify phase coherence and dissipation at final $g = g_f$, we perform simple sinusoidal fits $S(k, \tilde{\tau}) = S_f - S_o e^{-\tilde{\Gamma}_k \tilde{\tau}} - A_k e^{-\tilde{\Gamma}_k \tilde{\tau}} \cos(2\tilde{\tau} + \phi_0)$ to the data to extract (A_k, ϕ_0, $\tilde{\Gamma}_k$), as shown in Fig. 3(e-g) (the steady-state values S_f and S_o are not shown). The larger oscillation amplitudes A_k found in samples with $\Delta\tau \approx 1$ ms and 2 ms show that MI-induced quasiparticles are highly phase coherent. This can also be seen in the non-zero phase offset $\phi_0 \gtrsim \pi/2$ at $k \gtrsim 0.5/\mu$m in Fig. 3(f), which is coherently accumulated during the MI period. Furthermore, in Fig. 3(g), we observe a nearly constant decay rate $\tilde{\Gamma}_k \approx 0.31(8)$ at $k \gtrsim 0.8$ $/\mu$m for these MI-induced oscillations. This is close to the decay rate $\tilde{\Gamma}_k \approx 0.22(4)$ in samples without an MI period ($\Delta\tau = 0$), suggesting that the short MI dynamics does not heat up the sample significantly to increase the phonon dissipation rate.

We now focus on identifying a key signature of nonclassical correlations. To search for entanglement in the final phonon basis, we evaluate the squeezing parameter $C_k = \epsilon_k/\epsilon(k, g_f)$ at $g = g_f$ and plot the rescaled phonon spectra $\tilde{S}(k, \tilde{\tau}) = S(k, \tilde{\tau})/C_k$, as shown in Figs. 4(a-c) [35]. In this basis, the phonon spectra at momenta $k \gtrsim 1.5/\mu$m can be observed to oscillate above and below the rescaled quantum limit $\tilde{S} = 1$, showing signatures of two-mode squeezing and anti-squeezing as time evolves. The first minimum $\tilde{S}_{\min}$ identified at various momenta k is plotted in Fig. 4(d), in which we find that $\tilde{S}_{\min}$ violates the inequality Eq. (1) in a wider range for the MI sample with $\Delta\tau \approx 1$ ms than it does for the samples without

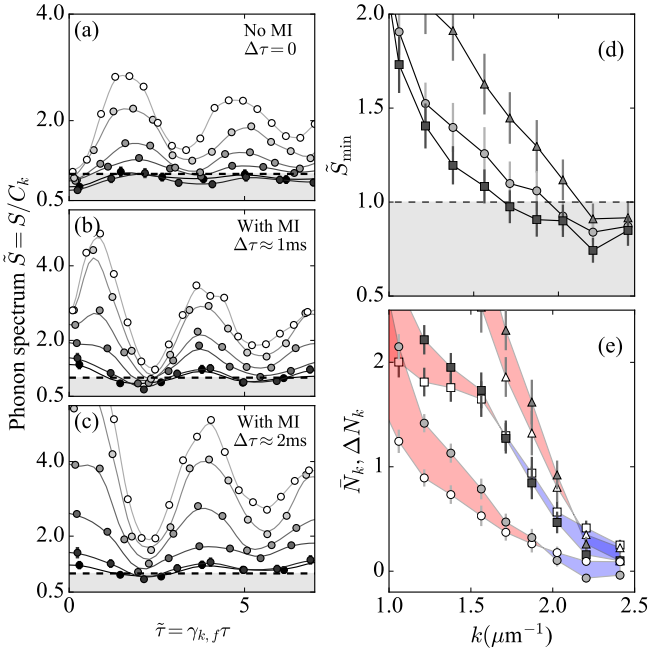

FIG. 4. Testing two-mode squeezing and quantum entanglement in the phonon basis. (a-c) Rescaled phonon spectrum $\tilde{S}(k, \tilde{\tau})$ for $k \approx (1.3, 1.6, 1.8, 2.1, 2.2, 2.4)/\mu$m (filled circles from bright to dark), evaluated using data as shown in Figs. 3(b-d). Solid curves are guides to the eye. (d) First minima $\tilde{S}_{\min}$ in the phonon spectra of various wavenumber k, at $\Delta\tau \approx 0$ ms (filled circles), 1 ms (squares), and 2 ms (triangles), respectively. In (a-d), horizontal dashed lines mark the quantum limit, below which Eq. (1) is violated. Error bars include systematic and statistical errors. (e) Mean phonon population $\bar{N}_k$ (filled symbols) and pair-correlation amplitude ΔN_k (open symbols) extracted using the first minima and maxima identified in (a, circles), (b, squares), and (c, triangles), respectively. Blue (red) shaded areas mark the region where $\Delta N_k > \bar{N}_k$ ($\Delta N_k < \bar{N}_k$). Error bars represent statistical errors.

MI or with longer $\Delta\tau$. The strongest violation is in the range of $2.1/\mu\text{m} \lesssim k \lesssim 2.2/\mu$m and has average $\tilde{S}_{\min} \approx 0.77(7) < 1$, compared to $\tilde{S}_{\min} \approx 0.84(8)$ without MI and $\tilde{S}_{\min} \approx 0.91(5)$ for $\Delta\tau \approx 2$ ms. Lastly, we comment that the initial violation of inequality for samples without MI at $\tilde{\tau} \approx 0$ is also clear. However, fewer modes show squeezing when the phonon spectra return back to the first minima $\tilde{S}_{\min}$.

To further interpret our result, we extract the mean phonon number $\bar{N}_k$ and the pair-correlation amplitude ΔN_k by using the first maximum $\tilde{S}_{\max}$ and minimum $\tilde{S}_{\min}$ identified in $\tilde{S}(k, \tilde{\tau})$ at each k in Figs. 4(a-c),

$$\bar{N}_k \approx \frac{\tilde{S}_{\max} + \tilde{S}_{\min}}{2} - 1$$
$$\Delta N_k \approx \frac{\tilde{S}_{\max} - \tilde{S}_{\min}}{2}. \quad (3)$$

As shown in Fig. 4(e), both $\bar{N}_k$ and ΔN_k have compa-

rably increased due to pair-production in MI samples of $\Delta\tau \neq 0$. Quantum entanglement appears to better prevail for $\Delta\tau \approx 1$ ms and at $k \gtrsim 1.5/\mu$m, where $\Delta N_k \gtrsim \bar{N}_k$. This may be understood as any excessive incoherent population $\bar{N}_k - \Delta N_k > 0$ in our samples can be due partially to quasiparticle dissipation during the quench and partially to incoherent (thermal) phonons present in the initial state. The latter are better suppressed at $k > 1.5/\mu$m as $\epsilon(k, g_i) > k_B T \approx \hbar \times 1$ kHz.

In summary, we observe pair-correlation signal and non-classical correlation in atomic quantum gases quenched to an attractive interaction, with two-mode squeezing $\tilde{S}_{\min} \approx 0.8 < 1$ below the quantum limit. Further reduction of initial incoherent phonon populations or of decoherence during pair-production processes may increase the non-classical signal in future experiments. Reaching $\tilde{S} < 0.5$ could open up applications requiring EinsteinPodolskyRosen entangled quasiparticle pairs [36–40]. Our method may be extended to analyze entanglement distribution between non-causal regions before the interaction quench. Furthermore, in analogy to the discussion in Ref. [41], extending our analyses of two-mode quadrature variance to skewness [42] and other higher-order correlation terms may provide necessary observables for probing entanglement entropy and transport in a quantum gas.

We thank M. Kruczenski and Q. Zhou for discussions. This work is supported in part by DOE QuantISED program (Grant # DE-SC0019202) and the W. M. Keck Foundation. C.-A.C. and C.-L.H. acknowledge support by the NSF (Grant # PHY-1848316).

* clhung@purdue.edu

[1] T. E. Keller and M. H. Rubin, Theory of two-photon entanglement for spontaneous parametric down-conversion driven by a narrow pump pulse, Physical Review A **56**, 1534 (1997).

[2] J.-W. Pan, Z.-B. Chen, C.-Y. Lu, H. Weinfurter, A. Zeilinger, and M. Żukowski, Multiphoton entanglement and interferometry, Reviews of Modern Physics **84**, 777 (2012).

[3] J. Eisert, M. Friesdorf, and C. Gogolin, Quantum many-body systems out of equilibrium, Nature Physics **11**, 124 (2015).

[4] S. Finazzi and I. Carusotto, Entangled phonons in atomic bose-einstein condensates, Physical Review A **90**, 033607 (2014).

[5] P. Jurcevic, B. P. Lanyon, P. Hauke, C. Hempel, P. Zoller, R. Blatt, and C. F. Roos, Quasiparticle engineering and entanglement propagation in a quantum many-body system, Nature **511**, 202 (2014).

[6] M. Cheneau, P. Barmettler, D. Poletti, M. Endres, P. Schauß, T. Fukuhara, C. Gross, I. Bloch, C. Kollath, and S. Kuhr, Light-cone-like spreading of correlations in a quantum many-body system, Nature **481**, 484 (2012).

[7] P. Calabrese and J. Cardy, Entanglement entropy and quantum field theory, Journal of Statistical Mechanics: Theory and Experiment **2004**, P06002 (2004).

[8] D. A. Abanin, E. Altman, I. Bloch, and M. Serbyn, Colloquium: Many-body localization, thermalization, and entanglement, Reviews of Modern Physics **91**, 021001 (2019).

[9] J. Steinhauer, Observation of quantum hawking radiation and its entanglement in an analogue black hole, Nature Physics **12**, 959 (2016).

[10] J. R. M. de Nova, K. Golubkov, V. I. Kolobov, and J. Steinhauer, Observation of thermal hawking radiation and its temperature in an analogue black hole, Nature **569**, 688 (2019).

[11] J. Hu, L. Feng, Z. Zhang, and C. Chin, Quantum simulation of unruh radiation, Nature Physics **15**, 785 (2019).

[12] J.-C. Jaskula, G. B. Partridge, M. Bonneau, R. Lopes, J. Ruaudel, D. Boiron, and C. I. Westbrook, Acoustic analog to the dynamical casimir effect in a bose-einstein condensate, Physical Review Letters **109**, 220401 (2012).

[13] C.-L. Hung, V. Gurarie, and C. Chin, From cosmology to cold atoms: observation of sakharov oscillations in a quenched atomic superfluid, Science **341**, 1213 (2013).

[14] M. Schemmer, A. Johnson, and I. Bouchoule, Monitoring squeezed collective modes of a one-dimensional bose gas after an interaction quench using density-ripple analysis, Physical Review A **98**, 043604 (2018).

[15] A. Rançon, C.-L. Hung, C. Chin, and K. Levin, Quench dynamics in bose-einstein condensates in the presence of a bath: Theory and experiment, Physical Review A **88**, 031601 (2013).

[16] K. E. Strecker, G. B. Partridge, A. G. Truscott, and R. G. Hulet, Formation and propagation of matter-wave soliton trains, Nature **417**, 150 (2002).

[17] J. H. Nguyen, D. Luo, and R. G. Hulet, Formation of matter-wave soliton trains by modulational instability, Science **356**, 422 (2017).

[18] P. Everitt, M. Sooriyabandara, M. Guasoni, P. Wigley, C. Wei, G. McDonald, K. Hardman, P. Manju, J. Close, C. Kuhn, *et al.*, Observation of a modulational instability in bose-einstein condensates, Physical Review A **96**, 041601 (2017).

[19] T. Mežnaršič, T. Arh, J. Brence, J. Pišljar, K. Gosar, Ž. Gosar, E. Zupanič, P. Jeglič, *et al.*, Cesium bright matter-wave solitons and soliton trains, Physical Review A **99**, 033625 (2019).

[20] J. Sanz, A. Frölian, C. Chisholm, C. Cabrera, and L. Tarruell, Interaction control and bright solitons in coherently-coupled bose-einstein condensates, arXiv preprint arXiv:1912.06041 (2019).

[21] C.-A. Chen and C.-L. Hung, Observation of universal quench dynamics and townes soliton formation from modulational instability in two-dimensional bose gases, Physical Review Letters **125**, 250401 (2020).

[22] Z. Tian, S.-Y. Chä, and U. R. Fischer, Roton entanglement in quenched dipolar bose-einstein condensates, Physical Review A **97**, 063611 (2018).

[23] J. Steinhauer, Measuring the entanglement of analogue hawking radiation by the density-density correlation function, Physical Review D **92**, 024043 (2015).

[24] A. Furusawa, J. L. Sørensen, S. L. Braunstein, C. A. Fuchs, H. J. Kimble, and E. S. Polzik, Unconditional quantum teleportation, Science **282**, 706 (1998).

[25] S. L. Braunstein and H. J. Kimble, Teleportation of continuous quantum variables, Physical Review Letters **80**,

869 (1998).
[26] A. I. Lvovsky and M. G. Raymer, Continuous-variable optical quantum-state tomography, Reviews of Modern Physics **81**, 299 (2009).
[27] See supplementary materials.
[28] A. J. Ferris, M. K. Olsen, E. G. Cavalcanti, and M. J. Davis, Detection of continuous variable entanglement without coherent local oscillators, Physical Review A **78**, 060104 (2008).
[29] L.-M. Duan, G. Giedke, J. I. Cirac, and P. Zoller, Inseparability criterion for continuous variable systems, Physical Review Letters **84**, 2722 (2000).
[30] R. Simon, Peres-horodecki separability criterion for continuous variable systems, Physical Review Letters **84**, 2726 (2000).
[31] S. Robertson, F. Michel, and R. Parentani, Controlling and observing nonseparability of phonons created in time-dependent 1d atomic bose condensates, Physical Review D **95**, 065020 (2017).
[32] S. Robertson, F. Michel, and R. Parentani, Assessing degrees of entanglement of phonon states in atomic bose gases through the measurement of commuting observables, Physical Review D **96**, 045012 (2017).
[33] C. Chin, R. Grimm, P. Julienne, and E. Tiesinga, Feshbach resonances in ultracold gases, Reviews of Modern Physics **82**, 1225 (2010).
[34] C.-L. Hung, X. Zhang, L.-C. Ha, S.-K. Tung, N. Gemelke, and C. Chin, Extracting density–density correlations from in situ images of atomic quantum gases, New Journal of Physics **13**, 075019 (2011).
[35] We note a ± 20 % variation of mean density across the analysis region (38×38 μm^2). As a result, the squeezing parameter C_k has at most a small $\pm 4\%$ variation relative to the mean within the reported momentum range as shown in Fig. 4.
[36] M. Reid and P. Drummond, Quantum correlations of phase in nondegenerate parametric oscillation, Physical Review Letters **60**, 2731 (1988).
[37] J. Peise, I. Kruse, K. Lange, B. Lücke, L. Pezzè, J. Arlt, W. Ertmer, K. Hammerer, L. Santos, A. Smerzi, *et al.*, Satisfying the einstein–podolsky–rosen criterion with massive particles, Nature communications **6**, 1 (2015).
[38] M. Fadel, T. Zibold, B. Décamps, and P. Treutlein, Spatial entanglement patterns and einstein-podolsky-rosen steering in bose-einstein condensates, Science **360**, 409 (2018).
[39] P. Kunkel, M. Prüfer, H. Strobel, D. Linnemann, A. Frölian, T. Gasenzer, M. Gärttner, and M. K. Oberthaler, Spatially distributed multipartite entanglement enables epr steering of atomic clouds, Science **360**, 413 (2018).
[40] K. Lange, J. Peise, B. Lücke, I. Kruse, G. Vitagliano, I. Apellaniz, M. Kleinmann, G. Tóth, and C. Klempt, Entanglement between two spatially separated atomic modes, Science **360**, 416 (2018).
[41] I. Klich and L. Levitov, Quantum noise as an entanglement meter, Physical Review Letters **102**, 100502 (2009).
[42] J. Armijo, T. Jacqmin, K. Kheruntsyan, and I. Bouchoule, Probing three-body correlations in a quantum gas using the measurement of the third moment of density fluctuations, Physical Review Letters **105**, 230402 (2010).